Solution Structure of Bromelain Inhibitor VI from Pineapple Stem: Structural Similarity with Bowman−Birk Trypsin/Chymotrypsin Inhibitor from Soybean[†,‡]

Ken-ichi Hatano,[§] Masaki Kojima,[§] Masaru Tanokura,[||] and Kenji Takahashi*[,§]

Department of Biophysics and Biochemistry, Faculty of Science, The University of Tokyo, Bunkyo-ku, Tokyo 113, Japan, and Biotechnology Research Center, The University of Tokyo, Bunkyo-ku, Tokyo 113, Japan

Received November 20, 1995; Revised Manuscript Received January 31, 1996[⊗]

ABSTRACT: Bromelain inhibitor VI from pineapple stem (BI-VI) is a unique double-chain inhibitor with an 11-residue light chain and a 41-residue heavy chain joined by disulfide bonds and inhibits the cysteine proteinase bromelain competitively. The structure of BI-VI in aqueous solution was determined using nuclear magnetic resonance spectroscopy and simulated annealing-based calculations. Its three-dimensional structure was shown to be composed of two distinct domains, each of which is formed by a three-stranded antiparallel β-sheet. Unexpectedly, BI-VI was found to share a similar folding and disulfide bond connectivities not with cystatin superfamily inhibitors which inhibit the same cysteine proteinases but with the Bowman−Birk trypsin/chymotrypsin inhibitor from soybean (BBI-I). BBI-I is a 71-residue inhibitor which has two independent inhibitory sites toward the serine proteinases trypsin and chymotrypsin. These structural similarities with BBI-I suggest that they have evolved from a common ancestor and differentiated in function during a course of molecular evolution.

Bromelain inhibitor VI from pineapple stem (BI-VI)[1] is one of seven isoinhibitors which inhibit cysteine proteinases, especially bromelain (Heinrikson & Kézdy, 1976). BI-VI consists of an 11-residue light chain and a 41-residue heavy chain cross-linked by five inter/intra-chain disulfide bonds (Hatano et al., 1995). The primary structure of BI-VI had, however, no similarities with those of the cystatin superfamily inhibitors which inhibit the same cysteine proteinases (Barrett et al., 1986). Especially, BI-VI does not contain the commonly conserved Gln-Val-Val-Ala-Gly sequence that exists as a probable binding site in most known cystatins (Bode et al., 1988). The secondary structure of BI-VI (Hatano et al., 1995) has also no homology with that of chicken egg white cystatin which was reported to consist of two α-helices and a five-stranded antiparallel β-sheet (Bode et al., 1988). Thus BI-VI is considered to be a unique cysteine proteinase inhibitor different from cystatin superfamily inhibitors.

In order to shed light on the structure−function relationship of BI-VI, we have determined its solution structure by NMR spectroscopy using a hybrid distance geometry/simulated annealing protocol. The results thus obtained led us to an unexpected finding that BI-VI is apparently homologous in three-dimensional (3D) structure with the Bowman−Birk trypsin/chymotrypsin inhibitor from soybean (BBI-I) which is a typical serine proteinase inhibitor. BBI-I is a single-chain molecule composed of 71 amino acids (Odani & Ikenaka, 1972) and strongly binds and inhibits trypsin and chymotrypsin at kinetically independent sites (Harry & Steiner, 1970). Previous NMR studies on BBI-I have shown that it has two distinct domains, each of which is comprised of a β-hairpin with a short segment making a third strand of antiparallel β-sheet (Werner & Wemmer, 1992). In the present paper, we report the 3D solution structure of BI-VI and compare it with the structure of BBI-I.

EXPERIMENTAL PROCEDURES

Materials. BI-VI was isolated and purified as described previously (Hatano et al., 1995). Peptide 4-methylcoumarin-7-amide (MCA) substrates and leupeptin were purchased from the Peptide Institute Inc., and chymotrypsin and trypsin were from Sigma Chemical Co.

NMR Measurements. The protein was dissolved in 100% D_2O or 90% H_2O/10% D_2O solutions at a concentration around 5 mM. The pH was adjusted to 3.9 using 1 M NaOD or DCl by use of a Radiometer PHM84 and an Ingold thin-glass electrode. ^{1}H NMR spectra were recorded on a Bruker AM-400 spectrometer at 40 °C or on a Bruker AMX-600 spectrometer at 30 °C.

Double-quantum-filtered correlation spectroscopy (DQF-COSY) (Rance et al., 1983), homonuclear Hartmann−Hahn spectroscopy (HOHAHA) (Bax & Davis, 1985), and nuclear Overhauser effect spectroscopy (NOESY) (Jeener et al., 1979; Macura et al., 1981) were recorded in the phase-sensitive mode (States et al., 1982). The water resonance was suppressed by irradiation during the relaxation delay. Two-dimensional spectra were recorded using a data size of

[†] This work was supported in part by Grants-in-Aid for Scientific Research from the Ministry of Education, Science and Culture of Japan and by a JSPS Fellowship for Japanese Junior Scientists to K.H.

[‡] The coordinates for the refined average structure and the 18 NMR structures have been deposited in the Brookhaven Protein Data Bank under the file names 1BI6 and 2BI6, respectively.

* To whom correspondence should be addressed. Present address: School of Life Science, Tokyo University of Pharmacy and Life Science, 1432-1 Horinouchi, Hachioji-shi, Tokyo 193-03, Japan. Tel.: +81-426-76-7146. Fax: +81-426-76-7149.

[§] Department of Biophysics and Biochemistry.

[||] Biotechnology Research Center.

[⊗] Abstract published in *Advance ACS Abstracts,* March 15, 1996.

[1] Abbreviations: BBI-I, Bowman−Birk inhibitor from soybean; BI-VI, bromelain inhibitor VI; Boc, *tert*-butyloxycarbonyl; DQF-COSY, double-quantum-filtered correlation spectroscopy; HOHAHA, homonuclear Hartmann−Hahn spectroscopy; MCA, 4-methylcoumarin-7-amide; NOE, nuclear Overhauser effect; NOESY, nuclear Overhauser effect spectroscopy; rms, root mean square; 3D, three dimensional; 2D NMR, two-dimensional nuclear magnetic resonance.

S0006-2960(95)02754-1 CCC: $12.00

512 (t_1) × 2048 (t_2) (512 × 4096 for DQF-COSY) with a spectral width of 6000 Hz. HOHAHA spectra were recorded with a mixing time of 46 ms. NOESY spectra were recorded with mixing times of 40, 60, 80, 120, and 200 ms at 40 °C and 100 ms at 30 °C. Before zero filling and double Fourier transformation, phase-shifted sine-bell functions (DQF-COSY) or Gaussian functions (HOHAHA and NOESY) were applied in both dimensions.

Spin system identification and sequential assignments were achieved in the normal manner as reported previously (Hatano et al., 1995).

Structure Calculations. Taking into account the spin diffusion and internal motion, intra- and interresidue distance constraints were derived from nuclear Overhauser effect (NOE) cross peaks in the NOESY spectra recorded with mixing times of 40 and 100 ms, respectively. The NOEs were classified as 1.8−2.7, 1.8−3.5, or 1.8−5.0 Å on the basis of cross-peak intensity. Standard values for pseudo-atom corrections were added to the NOE distance constraints where appropriate (Wüthrich, 1986). Cross peaks in the NOESY spectra were picked using the software package Felix (Biosym Technologies, Inc., San Diego, CA).

For 12 hydrogen-bonded amides, two additional distance constraints were defined, 2.5 Å ≤ $N_{(i)}$−$O_{(j)}$ ≤ 3.5 Å and 1.5 Å ≤ $NH_{(i)}$−$O_{(j)}$ ≤ 2.5 Å. Constraints on the ϕ angle were classified according to the size of the $^3J_{NH\alpha}$ coupling constant (Pardi et al., 1984). For the 18 residues whose $^3J_{NH\alpha} \geq 8$ Hz, ϕ was constrained to the range $-160° \leq \phi \leq -80°$; 6 residues had $^3J_{NH\alpha} < 7$ Hz and were constrained to $-100° \leq \phi \leq -20°$. Constraints on χ_1 were determined on the basis of the criteria of Wagner et al. (1987) by examination of DQF-COSY and NOESY spectra. From this analysis, three were constrained to $0° \leq \chi_1 \leq 120°$, one was constrained to $-120° \leq \chi_1 \leq 0°$, and four were constrained to $120° \leq \chi_1 \leq 240°$. The three *trans* ω angles for the X-Pro peptide linkages were constrained to 180° ± 10° according to Stewart et al. (1990). The structures were calculated using the program X-PLOR version 3.1 (Brünger, 1992) on an IRIS Indigo2 workstation (Silicon Graphics Inc.). The template structure was generated only with explicit disulfide bond constraints ($C_{\beta(i)}$−$S_{\gamma(j)}$ = 2.99 ± 0.05 Å and $S_{\gamma(i)}$−$S_{\gamma(j)}$ = 2.02 ± 0.05 Å) between $Cys3^{L(\text{light chain})}$ and $Cys7^{H(\text{heavy chain})}$, since BI-VI has a unique double-chain structure. Only this disulfide bond has been identified by chemical and enzymatic methods (Hatano et al., unpublished). The distance geometry embedding procedure was carried out followed by simulated annealing refinements as described before (Brünger, 1992). Computer graphic representations were obtained using the software package of MidasPlus (UCSF Computer Graphics Lab.) on the same workstation.

Assay of Inhibitory Activity toward Trypsin and Chymotrypsin. All enzymatic reactions were done at 25 °C. To a solution (1.485 mL) containing 1 nM preactivated enzyme and 10 μM inhibitor in 10 mM sodium acetate buffer at pH 4.6 was added 15 μL of 10 mM Boc (*tert*-butyloxycarbonyl)-Gln-Ala-Arg-MCA for trypsin or Boc-Ala-Ala-Pro-Phe-MCA for chymotrypsin in dimethyl sulfoxide. The increase of the fluorescence intensity was recorded at intervals of 10 s for 10 min. The amount of 7-amino-4-methylcoumarin produced by the action of trypsin or chymotrypsin was measured fluorometrically with an excitation wavelength of 370 nm and an emission wavelength of 460 nm in a Hitachi fluorescence spectrophotometer F-2000. We also performed the experiment using leupeptin as a control, which is a cysteine- and trypsin-like proteinase inhibitor. Leupeptin inhibited trypsin about 60% and did not inhibit chymotrypsin under these conditions.

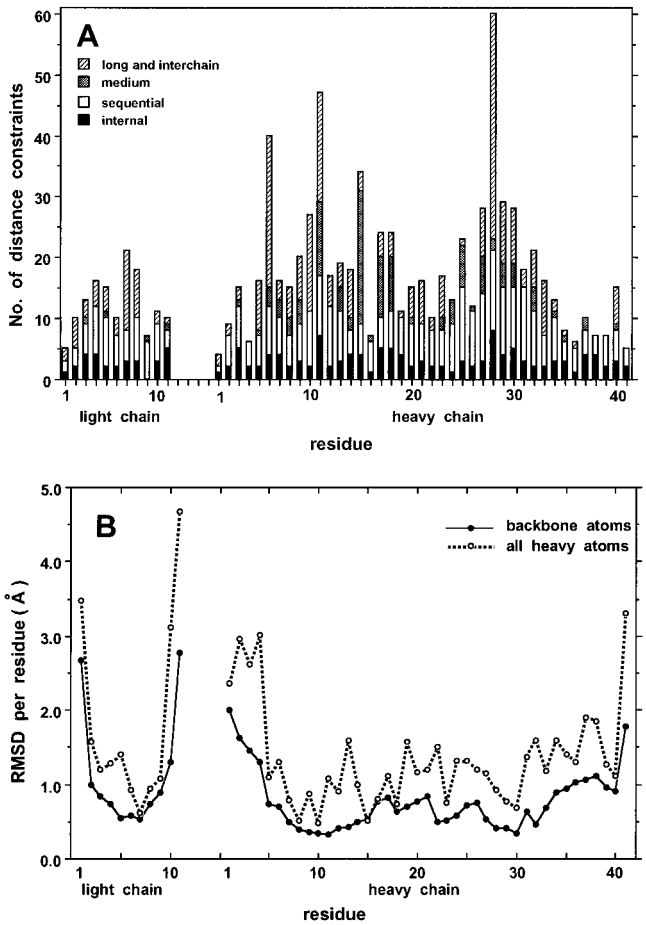

FIGURE 1: (A) Distribution of the number of experimental distance constraints on the primary sequence of BI-VI: filled bars, intraresidue NOEs; open bars, sequential NOEs; shaded bars, medium-range NOEs; hatched bars, long-range and interchain NOEs. (B) Distribution of the rms differences from the mean structure. The averaged values of backbone atoms (N, C_α, and C′) and all non-hydrogen atoms were plotted as filled and open circles, respectively.

RESULTS

Structure Calculations of BI-VI. A total of 539 NOE distance constraints were derived from assigned NOE cross peaks, which included 156 intraresidue, 166 sequential ($|i - j| = 1$), 60 medium-range ($1 < |i - j| < 5$), and 157 long-range and interchain ($|i - j| \geq 5$) constraints (Figure 1A). A total of 50 structures were calculated with X-PLOR using the hybrid distance geometry/simulated annealing protocol (Brünger, 1992) on the basis of the above distance constraints, 35 dihedral angle constraints, and 24 hydrogen bond distance constraints. Forty-two of them contained no distance violation greater than 0.5 Å and no dihedral angle violation greater than 5°. A final set of 18 structures was selected on the basis of minimum total energy. The 18 structures were averaged and restraint-minimized to give a mean structure. Structural statistics for the 18 converged and the mean structures are given in Table 1. Small root-mean-square (rms) deviations of the bonds from idealized geometry (typically <0.007 Å) as well as small values of the X-PLOR energies indicated good geometry of the final

Table 1: Structural Statistics of BI-VI

	18 structures	mean structure[a]
X-PLOR energies (kcal mol^{-1})		
E_{total}	132.1 ± 8.2	126.6
E_{VDW}[b]	6.6 ± 0.6	6.7
E_{CDIH}[c]	0.16 ± 0.19	0.01
E_{NOE}[d]	20.7 ± 4.8	18.6
rms deviation from idealized geometry		
bonds (Å)	0.0029 ± 0.0001	0.0029
angles (deg)	0.633 ± 0.008	0.629
impropers (deg)	0.377 ± 0.011	0.363
Cartesian coordinate rms differences (Å)	backbone atoms	all heavy atoms
BI-VI	0.98 ± 0.16	1.57 ± 0.14
BI-VI (2^L−10^L, 2^H−40^H)	0.75 ± 0.13	1.25 ± 0.14
A domain (9^H−29^H)	0.36 ± 0.05	0.87 ± 0.08
B domain (1^L−11^L, 1^H−7^H, 31^H−41^H)	1.15 ± 0.21	1.87 ± 0.19

[a] The mean structure was obtained by restrained minimization of the averaged coordinate of the individual 18 structures. [b] The X-PLOR F_{repel} function was used to simulate van der Waals interactions with atomic radii set to 0.8 times their CHARMm values (Brooks et al., 1983). [c] A force constant of 200 kcal mol^{-1} rad^{-2} was used for all torsional restraints. [d] A total of 538 NOE-derived distance restraints were applied with a square-well potential and a force constant of 50 kcal mol^{-1} Å^{-2}.

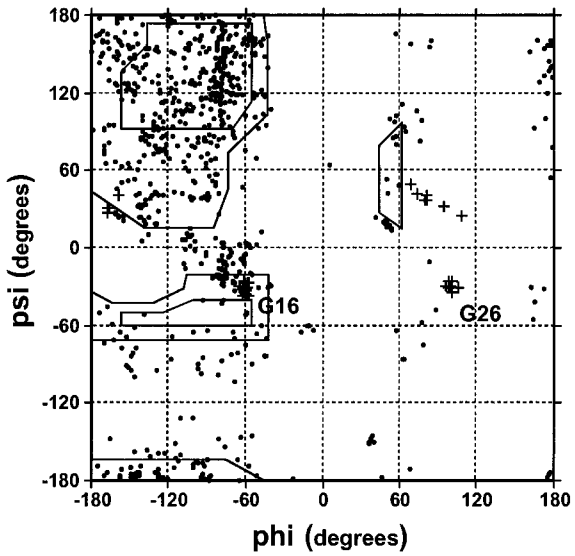

FIGURE 2: Ramachandran plot of the backbone conformational (ϕ, ψ) angles of the 18 final structures of BI-VI superimposed on the contours of the calculated energies for poly(L-Ala) (Brant & Schimmel, 1967). Glycine residues are plotted with + and labeled.

set of the structures. The 3D structure of BI-VI was well-defined except for the N-terminal and C-terminal parts (Figure 1B). The average rms differences (±standard deviation) of the well-defined region ($Ser4^L$ to $Cys8^L$, $Cys5^H$ to $Leu34^H$) were 0.46 ± 0.07 Å for the backbone atoms and 0.88 ± 0.08 Å for all heavy atoms; of the A domain ($Asp9^H$ to $Ile29^H$), these values were 0.36 ± 0.05 and 0.87 ± 0.08 Å, respectively (Figure 1B and Table 1). The quality of the solution structures was further assessed by a Ramachandran plot which provided distribution of dihedral backbone angles in the (ϕ, ψ) conformational space. Figure 2 shows the Ramachandran plot for the 18 converged structures of BI-VI. Most of the residues are located inside the low conformational energy regions, indicating that the converged structures are acceptable in view of the Ramachandran plot. From the further analysis of this plot, the residues of two three-stranded β-sheets in BI-VI were located on the B region, and those of a loop with $Pro15^H$ to $Lys19^H$ in BI-VI were on the A region. The region ($Pro15^H$ to $Lys19^H$) was considered to be a helical loop (Billeter et al., 1982). This is consistent with the results of circular dichroism measurements that indicated the content of α-helix to be about 10% (Hatano et al., 1995).

Disulfide Bonding of BI-VI. BI-VI contains ten cysteine residues, and the disulfide connectivities were determined as follows: $Cys3^L$-$Cys7^H$, $Cys6^L$-$Cys39^H$, $Cys8^L$-$Cys5^H$, $Cys14^H$-$Cys21^H$, and $Cys18^H$-$Cys30^H$ (Figure 3A) on the basis of NOEs between the β-methylene protons or between the α- and the β-methylene protons in these pairs of cysteines (Figure 4). These connectivities were confirmed by calculations without the explicit disulfide bond constraints. The final set of structures was calculated including these disulfide bond constraints. For the superposition of two average structures with and without such disulfide bond constraints, the average pairwise rms difference for all heavy atoms were 0.56 Å. The average structure without such disulfide bond constraints was calculated as described in Structure Calculations of BI-VI.

Description of the Tertiary Structure of BI-VI. The calculated 18 structures are shown in Figure 5A. The structure has two domains named A ($Asp9^H$ to $Ile29^H$) and B ($Glu1^H$ to $Cys7^H$, $Leu31^H$ to $Lys41^H$, and the light chain) (Figure 5B,C). Each domain is composed of an antiparallel three-stranded β-sheet, although each strand is very short (Figure 5D). Generally, a protein core tends to be occupied with some bulky hydrophobic side chains. However, the two disulfide bonds in the A domain and the three in the B domain seem to form the protein core (Figure 5C). This is consistent with the low values of solvent accessibility at cysteine residues (Hatano et al., unpublished). The disulfide cross-links appear to play a role of orienting these domains in proper conformation.

DISCUSSION

Determination of the disulfide bond arrangement in BI-VI led us to an unexpected finding that BI-VI is apparently homologous in structure with BBI-I. The primary structure of BI-VI, including the disulfide bond arrangement, is compared with that of BBI-I in Figure 3. In this comparison, the light and heavy chains of BI-VI are aligned in this order on the basis of the 3D structure of the inhibitor, in which the C-terminal $Arg11^L$ in the light chain is closely located to the N-terminal $Glu1^H$ (Figure 5), indicating that these two chains are linked in this order in the putative precursor form of BI-VI. On the other hand, the primary structure of BBI-I is shown in two different ways (Figure 3, panels B and C). In both cases, a remarkable homology was found between BI-VI and BBI-I, especially with respect to the disulfide bond arrangements. The distributions of the secondary structure elements in BI-VI (Hatano et al., 1995) are also similar to those in BBI-I (Werner & Wemmer, 1991). Thus, BI-VI seems to have two similar domains, named A and B domains like the two domains in BBI-I. $Leu10^L$ in the B domain of BI-VI appears to correspond to Leu43 in the antichymotryptic domain of BBI-I as shown in Figure 3A,B. Further, the sequence homology appears to be higher between the alignments in Figure 3, panels A and B, than those in Figure

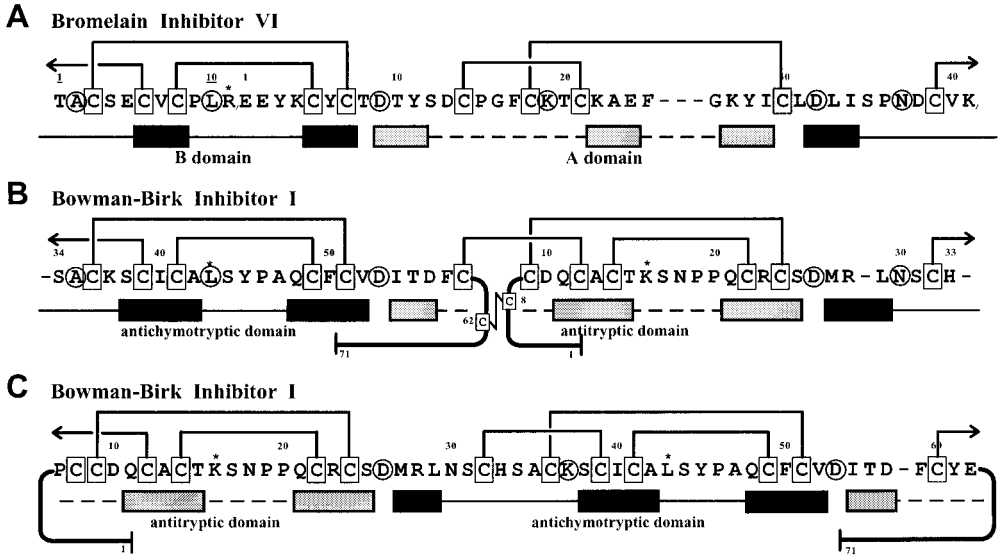

FIGURE 3: Alignments of BI-VI (Hatano et al., 1995) and BBI-I sequences (Odani & Ikenaka, 1972). Residues in the sequence of BI-VI are aligned in the order of the light chain and the heavy chain (A), while those of BBI-I are aligned so that the cysteine residues could correspond to those of BI-VI maximally (B and C). Sequences were aligned by hand. Identical residues are encircled except for cysteine residues. Disulfide bond arrangements are indicated with solid lines (Odani & Ikenaka, 1973). Those in BI-VI were determined by NMR. Stars above the sequences indicate a putative reactive site with bromelain ($Arg11^L$) in BI-VI or the reactive residues with trypsin (Lys16) and with chymotypsin (Leu43) in BBI-I. Distributions of the secondary structure elements are expressed as bars. Filled and shaded bars indicate the locations of the β-strand corresponding to the specific domains (Hatano et al., 1995; Werner & Wemmer, 1991).

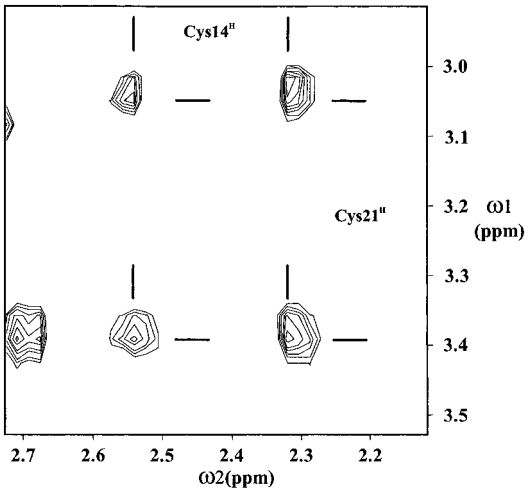

FIGURE 4: NOESY aliphatic region of BI-VI with a 200-ms mixing period in H_2O at 40 °C and pH 3.9. Assignments of NOEs between the β-methylene protons in $Cys14^H$ and $Cys21^H$ are illustrated.

3, panels A and C. Therefore, we tentatively assumed that the B and A domains in BI-VI correspond to the antichymotryptic and antitryptic domains of BBI-I, respectively, although the alternate possibility cannot be excluded.

The folding of the peptide chains in BI-VI was also found to closely resemble that in BBI-I (Werner & Wemmer, 1992); both proteins have two distinct domains, each composed of a three-stranded β-sheet (Figure 6). The A domain in BI-VI differs from the antitryptic domain of BBI-I in a few points. First, the A domain in BI-VI has no peptide bond discontinuity unlike the corresponding antitryptic domain in BBI-I (Figures 3A,B and 6). It is interesting to note that the structure of the terminal regions (Asp1 to Lys6 and Pro64 to Asn71) in BBI-I, which have no counterpart in BI-VI, is irregular as judged from the complete lack of any nonsequential interresidue NOEs (Werner & Wemmer, 1992). Second, the β-hairpin loop (containing a β-turn) of $Cys21^H$ to $Cys30^H$ in BI-VI is three residues shorter than that of Cys12 to Cys24 in BBI-I (Figures 3A,B and 6). The β-turn in the A domain is a two-residue type I′ turn ($Phe25^H$ and $Gly26^H$) (Hatano et al., 1995), while that in the antitryptic domain is a five-residue type VIb turn (Lys16 to Pro20) (Werner & Wemmer, 1991). The topology of the B domain in BI-VI and that of the antichymotryptic domain in BBI-I thus resemble each other except that the peptide chain is disconnected in the B domain at the ends of the light and heavy chains (Figure 3A).

BI-VI also inhibits trypsin weakly as previously reported for BI-VII, one of the seven bromelain isoinhibitors (Heinrikson & Kézdy, 1976). The A domain, however, has the short type I′ turn instead of the type VIb turn as described above. The pointed shape of the type VIb turns in BBI-I, observed also in the Kunitz and Kazal inhibitor families (Werner & Wemmer, 1992), represents the so-called "lock-and-key" motif that is thought to be the binding element of serine proteinase inhibitors (Laskowski & Kato, 1980). Therefore, the A domain is considered to be devoid of inhibitory activity toward trypsin or other proteinases due to the shortness of the reverse turn, the lack of the reactive Lys residue, and/or the lack of the third disulfide bond corresponding to Cys14-Cys22 in BBI-I which presumably maintains the site rigid enough to bind and inhibit serine proteinases (Figure 3A,B) (Werner & Wemmer, 1992).

On the other hand, the B domain has $Arg11^L$ as a putative reactive site for bromelain (Heinrikson & Kézdy, 1976). In this connection, it seems interesting to note that the cysteine proteinase inhibitor leupeptin from *Streptomyces* (Umezawa, 1976) has a sequence similar to the C-terminal region of the light chain (-$Leu10^L$-$Arg11^L$), which also has trypsin-inhibitory activity like BI-VI. The similarity between these inhibitors suggests that this portion may be primarily responsible for the weak inhibitory activity of BI-VI toward trypsin and that the $Leu10^L$-$Arg11^L$ sequence operates as a part of a substrate-like inhibitory reactive site with trypsin as well as with bromelain.

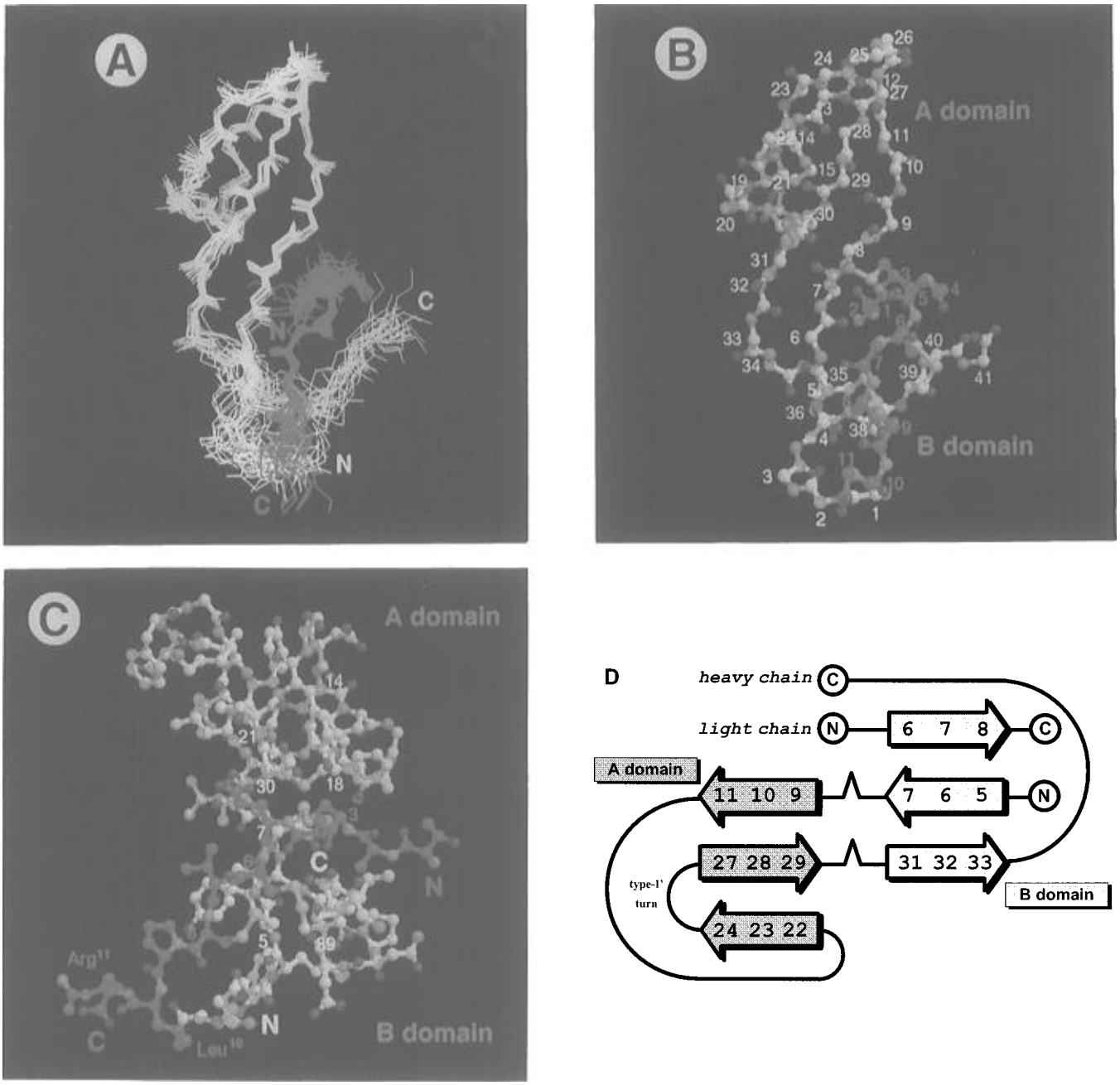

FIGURE 5: (A) Superposition of the backbone atoms (N, C_α, C′, and O) of 18 structures. The structures have been superimposed so as to minimize the rms differences from the mean structure for $Ser4^L$ to $Cys8^L$ and for $Cys5^H$ to $Leu34^H$. The light chain is in green and the heavy chain in white. The N- and C-termini are indicated by N and C, respectively. (B) A ball-and-stick representation of a selected structure closest to the average structure. The backbone atoms and disulfide bonds are shown. Carbon is in the color of each chain, oxygen in red, nitrogen in blue, and sulfur in yellow. All residues are numbered. (C) A ball-and-stick representation of the structure rotated 90° relative to the structure in (B). All heavy atoms are shown, and all cysteine residues are numbered. (D) Schematic drawing of the topology with the six β-strands depicted as arrows and the two bulges as nicks (Hatano et al., 1995). The numbers in the secondary structural elements indicate the residue numbers.

Interestingly, the $Leu10^L$ in BI-VI corresponds in position to the chymotrypsin-reactive residue Leu43 in BBI-I (Figure 3A,B). Therefore, the alignment suggests that BI-VI may also inhibit chymotrypsin. Indeed, we confirmed that BI-VI inhibits not only trypsin but also chymotrypsin although rather weakly; under the assay conditions used, BI-VI inhibited the activities of both trypsin and chymotrypsin about 20%. However, the B domain does not form a β-hairpin loop, unlike the antichymotryptic domain in BBI-I (Figures 3A,B and 6). This difference may account for the weak chymotrypsin-inhibitory activity of BI-VI; $Leu10^L$ may function weakly as the reactive residue for chymotrypsin.

As described above, the BI-VI molecule has many structural similarities, not to cystatin superfamily inhibitors (Bode et al., 1988) but to serine proteinase inhibitor BBI-I. These similarities argue strongly for the evolutionary relationship of BI-VI and BBI-I, suggesting that they share a common ancestor from which they have evolved. This is apparently in parallel with the supposition that serine and cysteine proteinases have evolved from the common ancestor (Bazan & Fletterick, 1988; Gorbalenya et al., 1989). During the course of molecular evolution, BI-VI might have acquired the $Leu10^L$-$Arg11^L$ sequence in the B domain and differentiated in function, while it appears to have lost the inhibitory

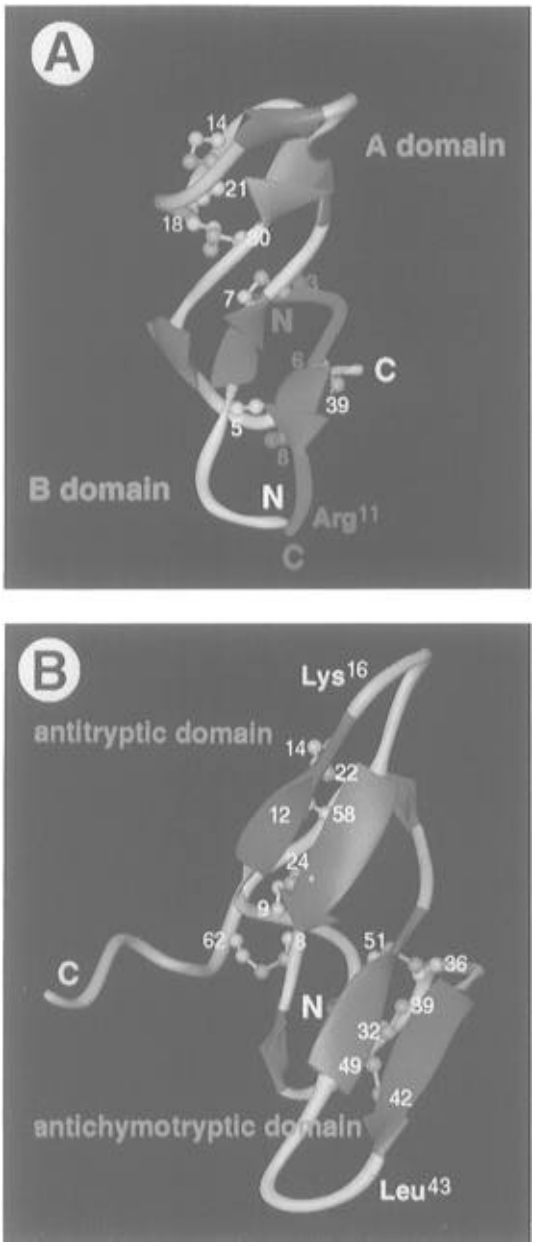

FIGURE 6: Comparison of the ribbon drawing structures of BI-VI and BBI-I. Cysteine residues are numbered at the positions of C_α, and their side chains are indicated with sticks and balls. Panels: (A) BI-VI (the selected structure); (B) BBI-I [Brookhaven Protein Data Bank 1BBI (Werner & Wemmer, 1992)].

function in the A domain. The A domain, however, seems to contribute to the conformational stability of the B domain. In the case of BBI-I, it was reported that when the antitryptic and antichymotryptic domains were proteolytically separated, the antichymotryptic domain retained only 20% of its activity, although the antitryptic domain retained 80% activity (Odani & Ikenaka, 1978). Therefore, both domains are needed for full inhibitory activity of BBI-I. This situation would also hold for the A and B domains in BI-VI (Table 1).

BI-VI is a unique double-chain inhibitor unlike other proteinase inhibitors including BBI-I which are single-chain inhibitors. Presumably, BI-VI is expressed as a single-chain precursor, which is then cleaved at the end of the light chain (Figure 3A) by a processing enzyme to form the unique double-chain structure. Very recently, we have isolated all major isoforms of bromelain inhibitors, which had homologous amino acid sequences; however, they all had a double-chain structure, and no single-chain inhibitor has been isolated (Hatano et al., unpublished).

ACKNOWLEDGMENT

We thank Prof. Sigeyuki Yokoyama (University of Tokyo) and Drs. Hiroshi Miyano and Ei-ichiro Suzuki (Ajinomoto Co., Ltd.) for the use of Bruker spectrometers and the late Mayumi Hatano and Dr. Yutaka Mutoh for their valuable advice in structural calculations and helpful discussions.

REFERENCES

Barrett, A. J., Fritz, H., & Turk, V. (1986) *Biochem. J. 236*, 312.
Bax, A., & Davis, D. G. (1985) *J. Magn. Reson. 65*, 355−360.
Bazan, J. F., & Fletterick, R. J. (1988) *Proc. Natl. Acad. Sci. U.S.A. 85*, 7872−7876.
Billeter, M., Engeli, M., & Wüthrich, K. (1982) *J. Mol. Biol. 155*, 321−346.
Bode, W., Engh, H., & Musil, H. (1988) *EMBO J. 7*, 2593−2599.
Brant, D. A., & Schimmel, P. R. (1967) *Proc. Natl. Acad. Sci. U.S.A. 58*, 428−435.
Brooks, B. R., Bruccoleri, R. E., Olafson, B. D., States, D. J., Saminathan, S., & Karplus, M. (1983) *J. Comput. Chem. 4*, 187−217.
Brünger, A. T. (1992) *X-PLOR Manual Version 3.1: A System for X-ray Crystallography and NMR*, Yale University Press, New Haven, CT.
Gorbalenya, A. E., Donchenko, A. P., Blinov, V. M., & Koonin, E. V. (1989) *FEBS Lett. 243*, 103−114.
Harry, J. B., & Steiner, R. F. (1970) *Eur. J. Biochem. 16*, 174−179.
Hatano, K., Kojima, M., Tanokura, M., & Takahashi, K. (1995) *Eur. J. Biochem. 232*, 335−343.
Heinrikson, R. L., & Kézdy, F. J. (1976) *Methods Enzymol. 45*, 740−751.
Jeener, J., Meier, B. H., Bachmann, P., & Ernst, R. R. (1979) *J. Chem. Phys. 71*, 4546−4553.
Laskowski, M., Jr., & Kato, I. (1980) *Annu. Rev. Biochem. 49*, 593−626.
Macura, S., Huang, Y., Suter, D., & Ernst, R. R. (1981) *J. Magn. Reson. 43*, 259−281.
Odani, S., & Ikenaka, T. (1972) *J. Biochem. (Tokyo) 71*, 839−848.
Odani, S., & Ikenaka, T. (1973) *J. Biochem. (Tokyo) 74*, 697−715.
Odani, S., & Ikenaka, T. (1978) *J. Biochem. (Tokyo) 83*, 747−753.
Pardi, A., Billeter, M., & Wüthrich, K. (1984) *J. Mol. Biol. 180*, 741−751.
Rance, M., Sørensen, O. W., Bodenhausen, G., Wagner, G., Ernst, R. R., & Wüthrich, K. (1983) *Biochem. Biophys. Res. Commun. 117*, 479−485.
Reddy, M. N., Keim, P. S., Heinrikson, R. L., & Kézdy, F. J. (1975) *J. Biol. Chem. 250*, 1741−1750.
States, D. J., Haberkorn, R. A., & Ruben, D. J. (1982) *J. Magn. Reson. 48*, 286−292.
Stewart, D. E., Sarker, A., & Wampler, J. E. (1990) *J. Mol. Biol. 214*, 253−260.
Umezawa, H. (1976) *Methods Enzymol. 45*, 678.
Wagner, G., Braun, W., Havel, T. F., Schaumann, T., Go, N., & Wüthrich, K. (1987) *J. Mol. Biol. 196*, 611−639.
Werner, M. H., & Wemmer, D. E. (1991) *Biochemistry 30*, 3356−3371.
Werner, M. H., & Wemmer, D. E. (1992) *Biochemistry 31*, 999−1010.
Wüthrich, K. (1986) *NMR of Proteins and Nucleic Acids*, John Wiley, New York.

BI952754+